

# VISION-BASED FIELD INSPECTION OF CONCRETE REINFORCING BARS

**Kevin Han, JunYoung Gwak & Mani Golparvar-Fard**

*University of Illinois at Urbana-Champaign, USA*

**Kamel Saidi, Geraldine Cheok, Marek Franaszek & Robert Lipman**

*The National Institute of Standards and Technology (NIST), USA*

**ABSTRACT:** Concrete reinforcing bars should be accurately placed in the positions shown on the construction drawings, adequately tied and supported before concrete is placed. These elements should be further secured against displacements within the tolerances recommended by project specifications. Ensuring compliance with contract documents and the building code applicable to the project under construction requires photographic documentation and close visual examination by field inspectors. Although inspection procedures are repetitive for every jobsite, the manual inspection methods are time-consuming and non-systematic. Moreover, the current practice of field inspectors walking into rebar cages and footings for close assessments can be a potential safety hazard on jobsites and can damage the integrity of the structure. To minimize the challenges of the current practice, this paper proposes a computer vision-based method for field inspection. In the proposed method, a field inspector can carefully walk around a rebar cage and take a complete collection of images from the underlying structure. Using a vision-based 3D reconstruction pipeline of Structure-from-Motion and Multi-view Stereo algorithms, a dense 3D point cloud model will be generated. Using an algorithm that maps and generates a density histogram of points, the locations and configuration of the rebars are identified. Finally, the spacings between rebars are calculated for field inspection. Experimental results on data collection, analysis, and visualization components of the proposed rebar inspection method is presented. These results show the promise of applying this low-cost approach in practice.

**KEYWORDS:** Rebar mapping, field inspection, vision-based 3D reconstruction, concrete placement

## 1. INTRODUCTION

To ensure compliance with contract documents and building codes, inspection of concrete reinforcing bars (rebars) prior to pouring concrete is required for every concrete structure. These elements should be accurately placed in the positions shown on the construction drawings and secured before concrete is placed. Inspection of rebars is largely done by visual examination of the layout pattern, of measuring the spacing, and of counting rebars (CRSI 2011). Considering the large size and the significant number of concrete placements for every project, this visual inspection - which is manually conducted by field inspectors - can be very time-consuming and inconsistent. In the current practice, a field inspector with a measuring tape walks around a rebar structure and often times pictures are taken to create a visual record of the as-built status. When measuring and counting rebars far away from the inspector, the numbers may be inaccurate and inconsistent due to physical limitations. Moreover, walking into rebar cages and climbing on column cages can be a potential safety hazard and can damage the integrity of the structure. The alternative method for inspecting large slabs is placing plywoods on the rebar structure as walking platforms. Although this method may be safer, the time and labor associated with moving the platforms are tedious. This can also damage the structural integrity and has a potential falling hazard as inspectors have to reach out and look down, standing on the edges of those plywoods. Figure 1 shows the current challenges associated with inspecting rebar structures. Since these visual inspections are repetitive for every jobsite, overcoming the current challenges discussed above can add value to the construction industry.

Possible visual sensing techniques that can help overcome these challenges are laser scanning and vision-based 3D reconstruction methods (Golparvar-Fard et al. 2012b). These methods can accurately create 3D point cloud models that can help determine the locations of rebars as well as spacings. Although the former is proven to be accurate and used in many incidences for quality control (Tang et al. 2011, Tang et al. 2010, and Akinici et al. 2006), it

---

Citation: Han, K. K., Gwak, J., Golparvar-Fard, M., Saidi, K. S., Cheok, G. S., Franaszek, M. & Lipman, R. R. (2013). Vision-based field inspection of concrete reinforcing bars. In: N. Dawood and M. Kassem (Eds.), Proceedings of the 13th International Conference on Construction Applications of Virtual Reality, 30-31 October 2013, London, UK.

requires an expert for operation, is very expensive, and is not mobile. The latter, however, can provide a low-cost solution to the industry as 1) consumer-level cameras or camcorders can be used, 2) calibration is not required, and 3) experts are not required for operation.



Fig. 1: a) An inspector measuring rebar spacings (Golparvar-Fard et al. 2010); and b) the safety hazard created through the density of the rebar layers for the inspector

This paper, therefore, presents a method for assessment of rebar spacing based on vision-based 3D point cloud models. In this approach, a 3D point cloud model is created from photos taken around a rebar structure. This model is then transformed to the site coordinate system using the coordinates of a set of target points placed on the structure prior to taking photos. An area selected for inspection is segmented from the site point cloud and the locations and configuration of rebars are automatically detected. Using coordinates of those detected rebars, spacings in all three directions ( $xyz$  in the Euclidean site coordinate system) are determined and represented. In the following sections, the paper presents 1) an overview of the current 3D reconstruction techniques that can be used for quality control, 2) research method using the techniques discussed in the previous section, 3) results of experiment, and 4) discussion on the contributions and practical benefits.

## 2. AN OVERVIEW OF AS-BUILT MODELING TECHNIQUES

### 2.1 Laser Scanner

Today, laser scanners can provide very accurate 3D spatial data that can make them suitable for quality control related tasks. There have been many studies that illustrate the use of laser scanners in the construction industry (Tang et al. 2011, Tang et al. 2010, and Akinci et al. 2006). Despite of its proven accuracy, there are still several practical limitations that needs to be addressed. Laser scanning takes time to set up and requires experts for operation. The more dominant laser scanner used these days on jobsites are also not mobile. If used for inspecting rebar configurations, in order to minimize occlusions happening in the lower layers of rebars, the laser scanning should be performed several times at different locations from different viewpoints. The size and the way laser scanning is performed limits such repetitive activities. The costs associated with laser scanners also can limit their use, as the costs of scanners and of operating experts are still high. Other limitations of laser scanning are mixed pixel phenomenon, range errors for thin structures, range jumps at reflectance and color boundaries, and large errors due to specular reflection (Golparvar-Fard et al. 2012 & 2011, and Tang et al. 2010).

### 2.2 Vision-based 3D Reconstruction

The vision-based 3D reconstruction has been significantly advanced in the computer vision domain in the last decade. This advancement was partly due to improved network bandwidths and servers, computer hardware, and digital photography at low cost. All these improvements allowed the handling of large numbers of high resolution images and points extracted from those images efficiently. With the help of these hardware advancement, researchers have developed algorithms that automatically detect features and match corresponding features from an unordered set of overlapping photos, which many readers may know as panoramic stitching algorithms. One example of such algorithms is Scale Invariant Feature Transforms (SIFT) (Lowe 2004). This algorithm is later combined with Structure-from-Motion (SfM) technique, which recovers camera parameters and reconstruct a sparse 3D point cloud model from matched points (Snavely et al. 2006). These methods combined with Multi-view Stereo (MVS) algorithms such as (Furukawa and Ponce 2010) – which require camera calibration information for

3D reconstruction – can produce dense point cloud models. These algorithms in the order of which they are discussed became a pipeline for constructing 3D models using unordered images. Golparvar-Fard et al. (2012 and 2011) and Saidi et al. (2011) has applied variants of this pipeline and generated as-built 3D point cloud models for progress monitoring and quality control purposes and have proven its accuracy compared to that of laser scanning techniques.

### 3. RESEARCH OBJECTIVES AND METHOD

The goal of this research is to prove the accuracy of the presented method and provide the industry with an automated method that can benefit from low-cost cameras and possibly replace the current practice (i.e., manually measuring and counting rebars and using expensive laser scanner). This research explores how the construction industry, specifically quality control practices, can benefit from low-cost computer vision techniques, such as 3D reconstruction using an unordered set of digital images.

#### 3.1 Setup and Data Collection

Before starting the inspection, a set of surveying targets are created and placed on the underlying structure of the rebars (See Figure 3). The site coordinates of these target points are extracted using conventional surveying techniques and will later be used to transform the reconstructed point cloud model from local coordinates into the site coordinate system. Once these targets are placed, the field engineer will walk around the rebar structure and will collect a large number of photos. These images and the coordinates of the targets are input to the algorithms. Here, it is assumed that the size of the rebar is known based on project specifications and the inspection task is mainly focused on assessing the spacing among the rebars.

#### 3.2 Algorithms: 3D Reconstruction and Extraction of Rebar Locations

Given a set of uncalibrated and unordered images of an underlying rebar structure, a dense 3D point cloud model can be generated using the pipeline, of the vision-based 3D reconstruction, discussed previously. This as-built 3D point cloud model – which has an unknown scale – needs to be transformed into the Euclidean site coordinate system. This similarity transformation has seven degrees-of-freedom (DOF):  $R$  for rotation (3 DOF),  $T$  for translational offset (3 DOF), and  $S$  for a uniform scale (1 DOF) and can be represented as:

$$\begin{bmatrix} X_{site} \\ 1 \end{bmatrix}_{4 \times 1} = \begin{bmatrix} sR & T \\ 0 & 1 \end{bmatrix} \begin{bmatrix} X_{local} \\ 1 \end{bmatrix}_{4 \times 1} \quad (1)$$

where  $X_{site}$  and  $X_{local}$  represent the coordinates of points in site and local coordinate systems respectively. By selecting three points from both local and site coordinate systems, these seven unknowns can be calculated. Because the coordinates of these points are manually collected, there could be potential errors when transforming. Particularly there could be a user selection error due to the difficulty of choosing points with the naked eyes from the reconstructed point cloud model. Moreover choosing a minimum number of points that are relatively close to each other may not best represent the entirety of the point cloud for calculating the transformation. This is due to potential amplification when scaled up the entire model. Taking these into consideration, more target points at longer distances from each other could be selected to minimize the registration error. This can be represented in form of minimization of the sum of the squared errors as follows:

$$\sum_1^n \|e_i\|^2 = \sum_1^n \|\Psi_{site,i} - sR(\Psi_{local,i}) - T\|^2 \quad (2)$$

where  $\Psi_{site,i}$  and  $\Psi_{local,i}$  represent the coordinates of the targets in site and local coordinate systems respectively. To solve this equation, similar to Golparvar-Fard et al. (2009), Horn's (1987) closed-form solution to the least square problem of absolute orientation is used. Once the similarity transformation is calculated, using Eq. 1, the point cloud is transformed into the site coordinate system. To extract the locations of the rebar, one important assumption can be made based on the typical characteristics of rebar structures: rebars are mainly oriented in two orthogonal directions. Based on this assumption, similar to Saidi et al. (2011), the following steps are conducted to automatically extract the potential locations of the rebar: After the region of interest for inspection is segmented from the point cloud model, all the points are projected onto the Z-axis (vertical) and a density histogram of those points is generated. This histogram indicates the locations of each rebar layer in the Z direction (see Figure 5a).

Next, the point cloud in each separated layer is quantized into smaller volumes of subspaces (voxels) wherein for each voxel, it is assumed that the orientation of the rebar layer stays constant. For each voxel, all the points are projected onto the  $X$  and  $Y$  axes independently and density histograms representing the occupancy density of points along each axis are generated. For each histogram, the maximum peaks which represent the centerlines of rebar are identified. Here, a point  $x$  in the histogram is considered a maximum peak if it simply has the maximal value compared in the close neighborhood of the point. Once the locations of rebars for each voxel are identified, they are connected to form the entirety of the model and the center-to-center spacing between two adjacent rebars can be calculated. Figure 2 illustrates the process model for this method.

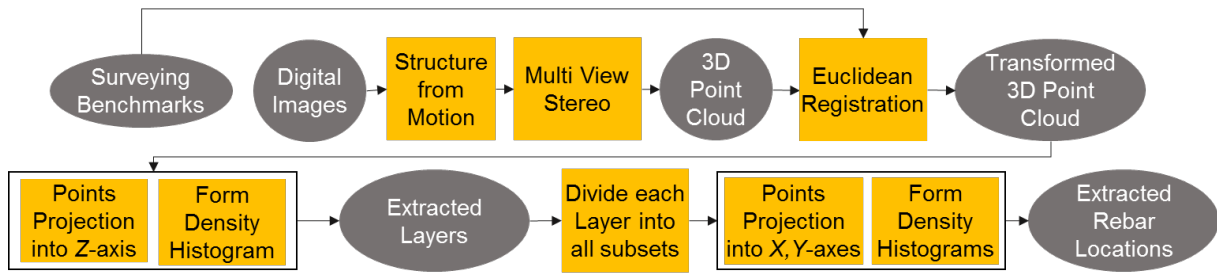


Fig. 2: The process model for the proposed method.

## 4. EXPERIMENT

### 4.1 Data Collection and Setup

The data for this research was acquired from an experiment conducted at the National Institute of Standards and Technology (NIST)'s Intelligent and Automated Construction Job Site (IACJS) testbed. The reconfigurable rebar cage was fabricated as a mockup of a typical type of rebar cage. The epoxy-coated #6 rebars are spaced at 15.2 cm and the cage consists of two layers of rebars, separated by approximately 30.5 cm. Each layer consists of thirteen 3.66 m long rebars laid on top of twenty-two 15.2 cm long rebars. To complicate the problem and embrace the real world challenges, three pipes are inserted in between the two layers, as can be seen in Figure 3. To minimize the registration error, fifteen targets were placed on the rebars as the control points. The global coordinates of these targets in the site coordinate system were retrieved using an Indoor Global Positioning System (iGPS) instrument. These coordinates were later used when transforming the point cloud to the site coordinate system. The iGPS system installed in the IACJS Testbed has a 3D position uncertainty of  $\pm 0.250$  mm and a maximum range between a receiver/transmitter pair of 40 m.

Photos were taken with a commercially available digital single lens reflex camera (DSLR). The pictures are originally taken with the spatial resolution of approximately 21.1 megapixels. Then, they were downsampled to 7.6 megapixels to match the common spatial resolution for the cameras in the recent smartphones. About 850 images were taken - later subsampled into smaller numbers of images. To minimize visual occlusion in the lower layer, a field engineer walked around the cage and took about one image per linear foot. To capture the detailed images of the center of the cage, about 50 to 70 images were taken from the top. See Figure 3 for examples of images of the cage and targets.



Fig. 3: The images of the rebar cage and targets used for 3D reconstruction.

### 4.2 Sensitivity Analysis and Discussion on the Experimental Results

#### 4.2.1 3D Point Cloud Modeling

To test sensitivity to the number of images used for reconstruction, a subset of 100, 150, 200, and 250 images were randomly chosen. To ensure that these images were being evenly chosen throughout the structure, the structure was divided into several subareas in  $x$ - $y$  plane. For each subarea, the visibility of points from cameras was calculated based on back-projection of each point into all cameras and checking the visibility constraints with respect to camera's field of view. This information was available as part of the outcome of the SfM algorithm. Then cameras based on their contribution to the overall 3D reconstruction were uniformly subsampled. This approach also coincided with the data collection method of a field engineer walking around the structure taking photos. For each subset of images, a 3D point cloud model was generated using the pipeline of the 3D reconstruction algorithm as discussed previously. These models were trimmed for the inspection stage. Figure 4 and Table 1 show the relationship between the density and completeness of these models with respect to the number of images used.

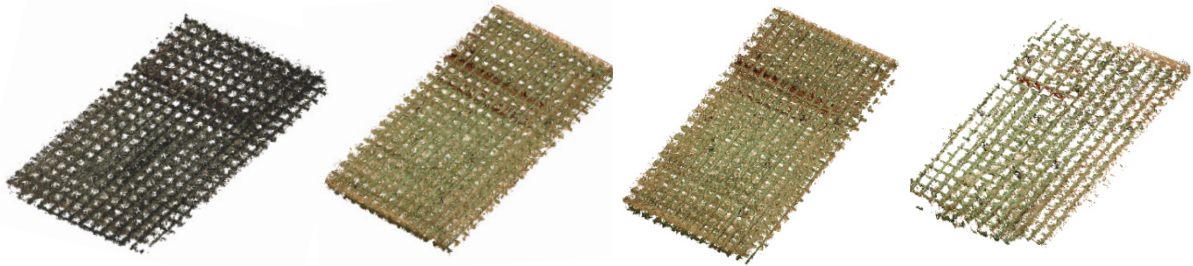


Fig. 4: 3D point cloud models from a) 250, b) 200, c) 150, and d) 100 images

Table 1: Number of points generated from each sample

# of Images	250	200	150	100
Density of the point cloud	13,320,977	10,696,247	11,554,036	1,046,101

#### 4.2.2 Extracting Rebar Locations from Density Histogram

All the points in the reconstructed models were projected onto the  $Z$ -axis perpendicular to the rebar plane ( $X$ - $Y$ ). The result is illustrated in Figure 5a. As can be easily observed, the two major peaks in red boxes indicate the locations of the top and bottom rebar layers in the  $Z$ -axis. The top and bottom layers consist of two layers of rebars each – longitudinal and transverse rebars and the two local peaks within each box represent these two layers. Once the locations of each layer in  $Z$ -axis were determined, the points were projected onto the other axes and the density histograms were plotted. When projecting all the points, for instance, to  $X$ -axis, some information in the projected axis may be missing. For example, if one rebar was bent in a certain location, that bending will not be captured because the algorithm only shows a unique location for that section of the rebar which in this case is represented with the location with most points. To deal with this problem, as mentioned previously, the rebar cage was subdivided into voxels and the points in each voxel were projected for plotting the histograms, assuming that the rebars are rigid enough to be straight within the chosen range – 50 cm in this case (see Figure 6). Even if there is any physical damage (i.e. bent rebars), the location with most points will be relatively close to the actual location of the rebar within that small range. The shorter length can be used for finer detection of the locations but there is a risk of more points from instrument noise than points from rebars in some regions as the length decreases. For the given dataset, a length of 30 cm seemed to work. Figure 5b illustrates the density histogram of one voxel and Figure 6 illustrates how the cage was subdivided and analyzed.

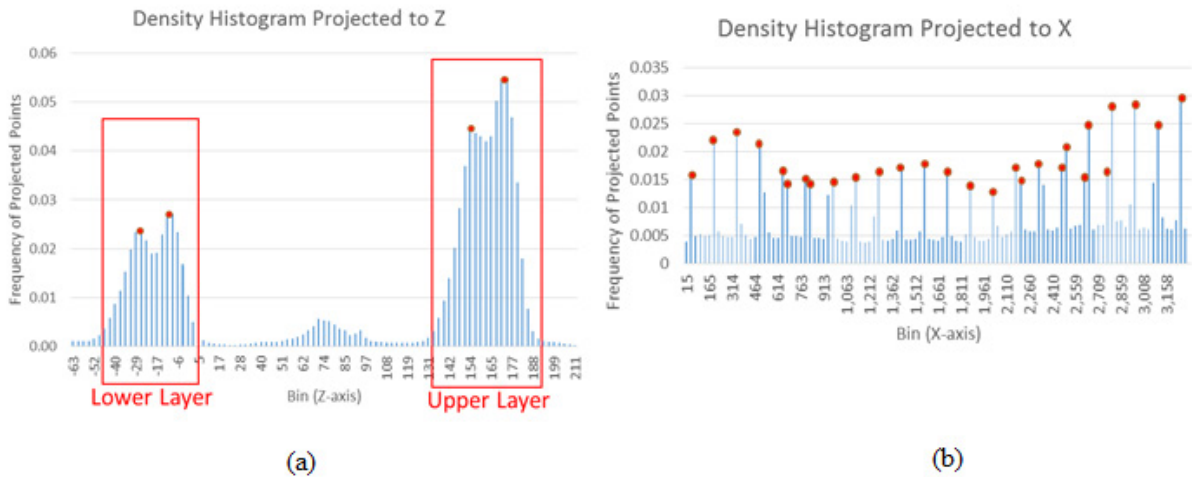


Fig. 5: Examples of Density Histogram of Points Projected to (a) Z-axis and (b) to X-axis.

The red dots in Figure 5 indicates the potential locations of the rebars and the unevenly spread dots in some areas may be an indication of the noise in the data. These red dots from the noise were ignored by comparing the possible rebar locations in one segment with the locations in the other segments. Because a rebar will be almost always straight within a short length (i.e. 50 cm) unless its configuration is significantly irregular, any outliers can be ignored. Lastly, the density histograms of the points projected onto the Z-axis for every 50 cm × 50 cm are plotted to capture more accurate locations of Z-coordinates throughout the structure. Figure 8 illustrates the intersections of the rebars and shows how the rebars are deflected towards the center of the rebar cage. Note that Z-axis is exaggerated for the illustration purpose.

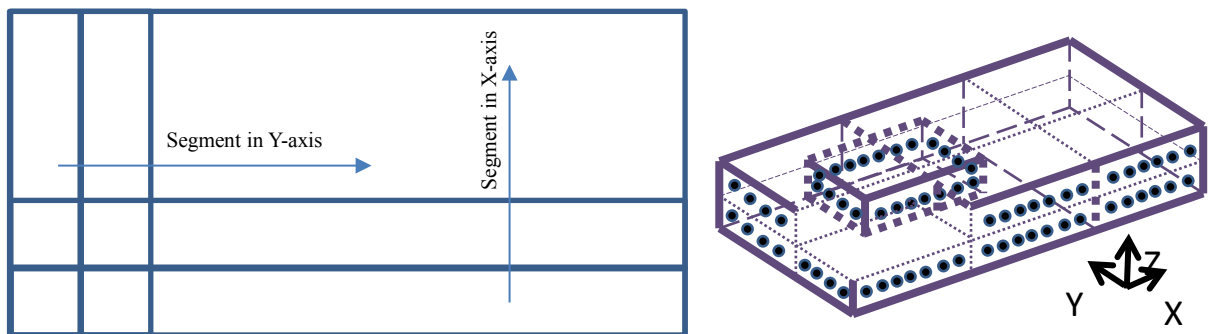


Fig. 6: Illustration of how the rebar cage is segmented: top view on left and 3D view on right.

#### 4.2.3 Validation

A 3D point cloud model generated from a laser scanner was used for 1) validating the accuracy of the 3D

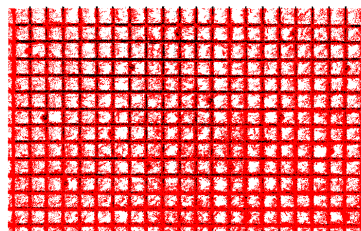


Fig. 7: Superimposed point cloud models (red: vision-based reconstruction and black: laser scanning)

reconstruction and 2) running the same algorithms with the laser scanned model to test which of those two 3D models provides a better result. The accuracy of 3D reconstruction was tested by Golparvar-Fard (2012b) and the registration error was less than 1 mm registration error when 15 targets were used by comparing it to a BIM model. For this reason, this research only tested the accuracy of the point cloud model by superimposing it into the point

cloud model of the laser scanner and visually examining the results of 3D reconstruction. As seen in Figure 7, the accuracy of the vision-based reconstruction looks promising.

The extracted locations of the rebars are plotted in 2D (top view) and 3D and displayed in Figure 8 and 9, respectively. Figure 8a illustrates the results from the laser scanner and Figure 8b illustrates the results from the vision-based 3D reconstruction using 200 images. Because the laser scanning was performed once, it had limited visibility, which is why some of the rebars in the lower layer were not detected due to occlusions of the inserted pipes. On the other hand for the vision-based approach, every rebar was successfully detected as it used images taken from different perspectives which minimized the chance of occlusion. As the number of images decreased, the occlusions became apparent (see Figure 10). Notice the upper layer that is always free from occlusion and almost always detected all the rebars in all cases, whereas the lower layer with occlusions was very sensitive to the number of input images. More images meant less occlusion as more viewpoints became available.

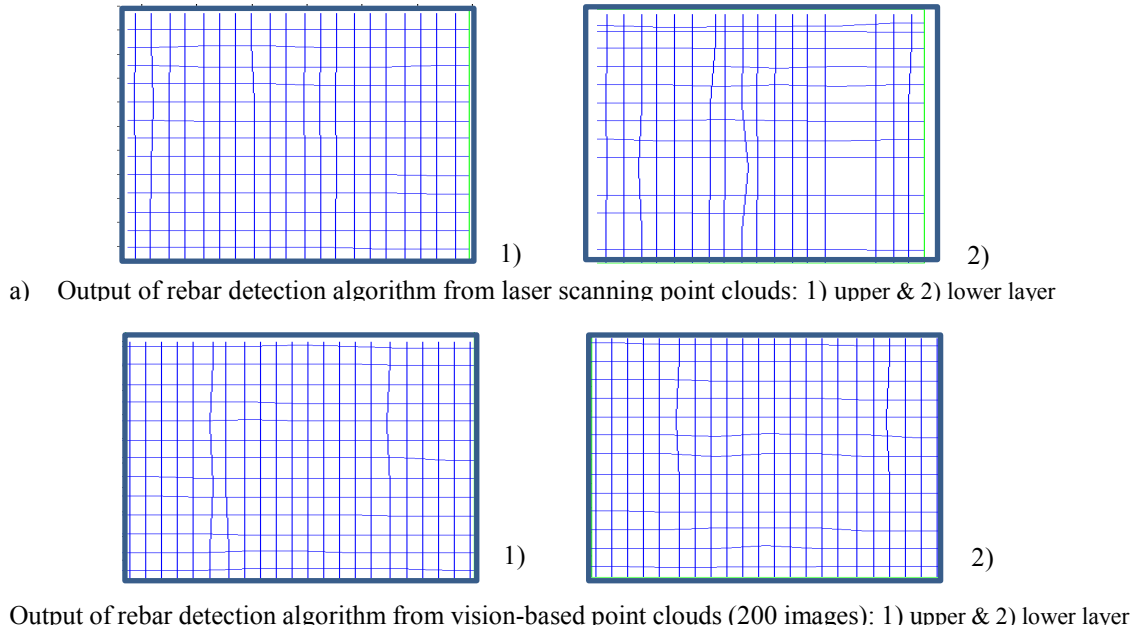


Fig. 8: Detected rebar layouts for laser scanner (top) and vision-based (bottom).

Since the rebars are only supported around the edges of the cage by the formwork, there is deflection towards the center of the cage and this was also successfully captured as illustrated in Figure 9. Partial rebar spacing is given in Table 2 due to space constraint. The results look promising when compared to the actual spacing of 15.2 cm, considering that there could be small error in placement of the rebars into the cage. All the results for the vision-based reconstruction using 250 and 200 images were within the tolerance of 7.6 cm to 10.2 cm (3 in to 4 in) defined by ACI 117 (CRSI 2011). Notice that the  $z$ -coordinate is determined and assigned for each  $50\text{cm} \times 50\text{cm}$  subarea. This is acceptable since deflections are so small that it is even hard to see the actual deflections with eyes. The largest deflection (difference between the highest and the lowest  $z$ -coordinate) was 1.5 cm. For more accurate distribution of  $z$ -coordinates, the size of the subarea can be decreased but not smaller than  $30\text{cm} \times 30\text{cm}$  by the authors' experience.

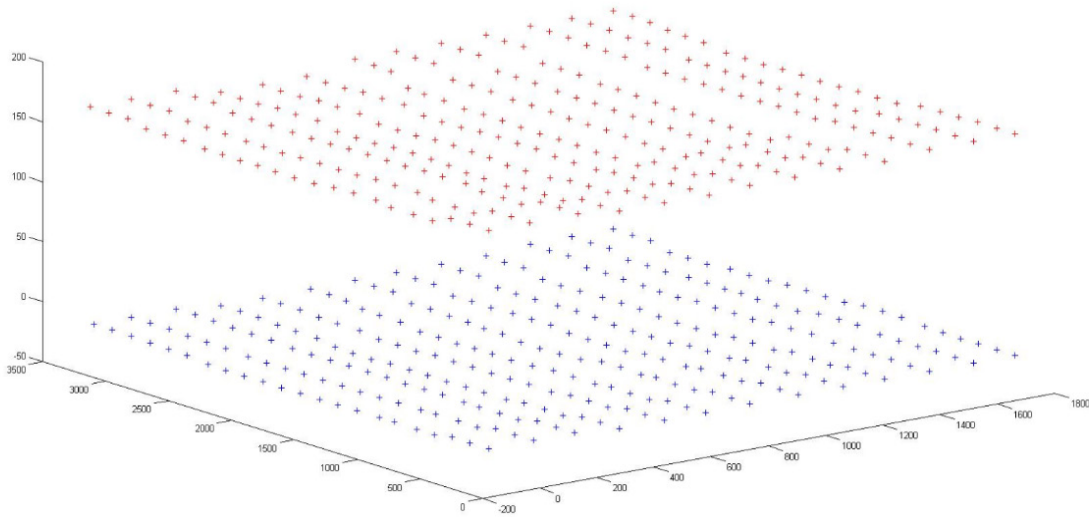


Fig. 9: Plotted rebar intersections.

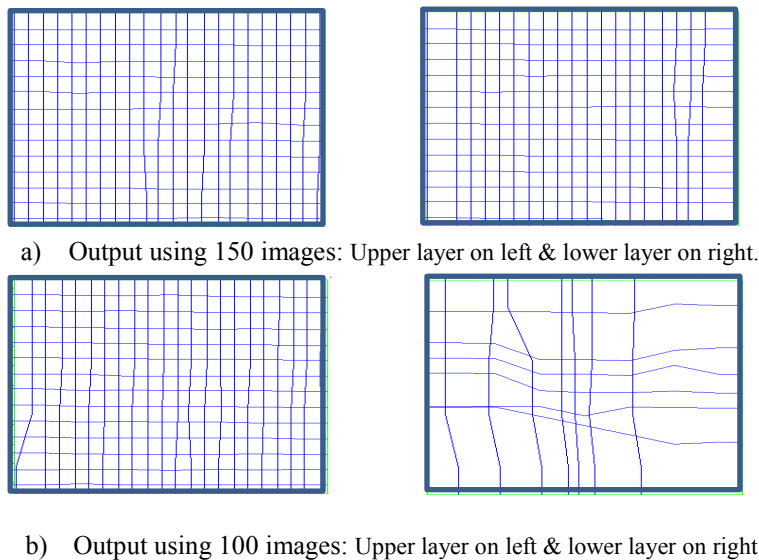


Fig. 10: Output from vision-based reconstruction

Table 2: Spacing output from the vision-based reconstruction using 200 images. First 13 results of the second line from the bottom in *x*-direction.

Lower (cm)	15.6	14.4	15.6	15.6	14.4	15.6	16.8	15.6	14.4	15.6	15.6	14.4	15.6	14.4
Upper (cm)	14.4	16.8	14.4	15.6	15.6	14.4	15.6	15.6	15.6	15.6	15.6	14.4	14.4	16.8

This research can potentially be used in conjunction with the 4-dimensional augmented reality (D<sup>4</sup>AR) modeling which Golparvar-Fard (2012) has developed for progress monitoring. In that system, an as-built point cloud model is generated from images and superimposed with IFC-based Building Information Models (see Figure 11). A rebar structure in that point cloud model for progress monitoring can be segmented and inspected at the same time. With more photos for denser and accurate 3D reconstruction, this system can also perform quality control related tasks, such as checking rebar spacing.

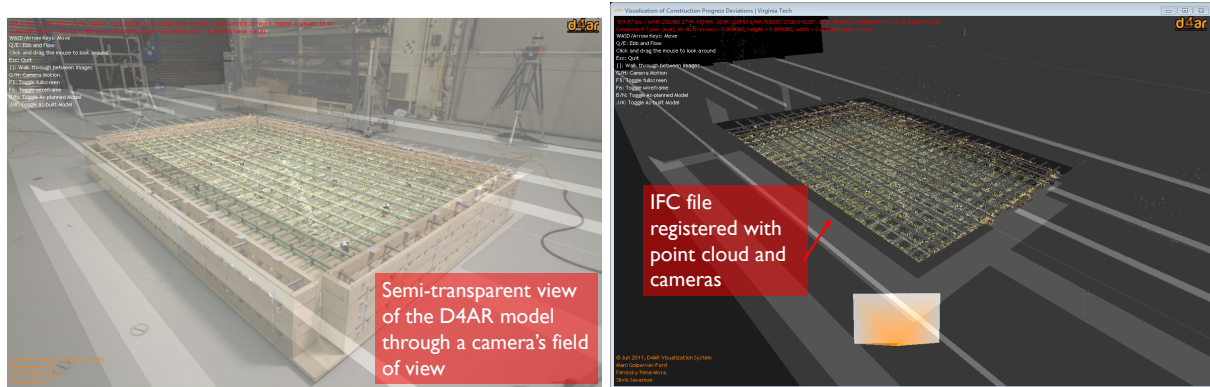


Fig. 11: The cloud model superimposed with IFC-based BIM model via the D<sup>4</sup>AR

## 5. CONCLUSION AND FUTURE RESEARCH

This paper presented the vision-based field inspection of rebars for concrete slab structures. The results of this research show how digital images can provide the detailed information that can be used for quality control. The results also prove the accuracy of such information is even comparable to that of the laser scanning method. It was shown that this vision-based approach using the images yielded better results than using the laser scanner in the presence of occlusion. It was also shown that the number of images had a great impact on the quality of the 3D reconstruction and therefore on the quality of the rebar detection. The results show that the vision-based approach using digital images can provide low-cost field inspection and has the potential to replace the current labor-intensive and unsafe visual examination, measuring and counting of each and every rebar.

Inspecting more complex structures in an uncontrolled environment will be studied in future work. This study can also expand to inspecting lap slices, stirrups, and rebar cages with more irregular configuration. The geometry fitting into possible rebar locations shown by peaks in density histograms will be studied. This can improve the process of choosing inliers against possible outliers. This approach can detect lap splices as it will search for cylinders in a given range around each location of the peaks and can also differentiate between sizes of rebars by fitting different size cylinders. The main goal is to automate and expedite the whole inspection process, which eventually can eliminate idle time prior to pouring concrete. These are all being explored as part of an ongoing research project and results are forthcoming.

## 6. ACKNOWLEDGEMENT

The authors would like to thank the support and help of C. Brown, J. Swerdlow, I. Katz of NIST and B. Ghadimi, and M. Akula with data collection and experimental setup.

## 7. REFERENCES

- Akinci B., Boukamp F., Gordon C., Huber D., Lyons C., and Park K. (2006). A Formalism for Utilization of Sensor Systems and Integrated Project Models for Active Construction Quality Control, *Automation in Construction*, Vol. 15, No. 2, February, 2006, pp. 124--138.
- Casey M. J. and Urgessa G. S. (2013). Rebar Cage Construction and Safety: Best Practices, *Construction Institute*, American Society of Civil Engineers.
- Concrete Reinforcing Steel Institute (CRSI) (2011). Field Inspection of Reinforcing Bars, *CRSI Technical Note CTN-M-1-11*, Concrete Reinforcing Steel Institute.
- Furukawa Y. and Ponce J. (2010). Accurate, Dense, and Robust Multi-view Stereopsis. *IEEE Trans. Pattern Analysis and Machine Intel.* 32, 1362–1376.
- Golparvar-Fard M., Peña-Mora F., and Savarese S. (2012a). Automated Progress Monitoring Using Unordered Daily Construction Photographs and IFC-Based Building Information Models, *J. Comput. Civ. Eng.*, 10.1061/(ASCE)CP.1943-5487.0000205 (Feb. 11, 2012).

- Golparvar-Fard M., Ghadimi B., Saidi K., Cheok G., Franaszek M., and Lipman R. (2012b). Vision-based 3D Mapping of Rebar Location for Automated Assessment of Safe Drilling Areas Prior to Placing Embedments in Concrete Bridge Decks, *Construction Research Congress 2012*: pp. 960-970.
- Golparvar-Fard M., Bohn J., Teizer J., Savarese S., and Peña-Mora F., (2011), Evaluation of Vision-based Modeling and Laser Scanning Accuracy for Emerging Automated Performance Monitoring Techniques, *J. of AutoCon*, 20(8), 1143-115.
- Golparvar-Fard, M.U, Fukuchi, Y., Peña-Mora, F., and Savarese, S. (2010). "D<sup>4</sup>AR – 4D Augmented Reality – Models for As-built Visualization and Automated Progress Monitoring of Civil Infrastructure Projects." *Proc., 10th Int. Conference on Construction Applications of Virtual Reality 2010*, Sendai, Japan, Nov 4-5.
- Golparvar-Fard M., Peña-Mora F., & Savarese S. (2009). D4AR - A 4-Dimensional Augmented Reality Model for Automating Construction Progress Data Collection, Processing and Communication. *J. of ITCOn*, 14, 129-153.
- Horn, B. (1987). Closed-form Solution of Absolute Orientation using Unit Quaternions. *J. of the Optical Society, A(4)*, 629-642.
- Lowe D. (2004). Distinctive Image Features from Scale-invariant Keypoints. *Int. J. of Computer Vision*, 60(2), 91-110.
- Saidi K., Cheok G., Franaszek M., Brown C., Swerdlow J., Lipman R., Katz I., Golparvar-Fard M., Goodrum P., Akula M., Dadi G., and Ghadimi B. (2012), "Development and Use of the NIST Intelligent and Automated Construction Job Site Testbed". *NIST TN 1726*, National Institute of Standards and Technology, Gaithersburg, MD, Dec, 2011.
- Snavely N., Seitz S. M., and Szeliski R. (2006). Photo Tourism: Exploring Photo Collections in 3D. *ACM Transactions on Graphics (Proceedings of SIGGRAPH 2006)*, 25(3), pp. 835-846, 2006.
- Tang P., Huber D., and Akinici B. (2011). Characterization of Laser Scanners and Algorithms for Detecting Flatness Defects on Concrete Surfaces, *J. Comput. Civ. Eng.*, 25(1), 31–42.
- Tang P., Huber D., Akinici B., Lipman R., and Lytle A. (2010). Automatic Reconstruction of As-built Building Information Models from Laser-scanned Point Clouds: a Review of Related Techniques, *J. of AutoCon*, 19, 829-843.